MOLECULAR AND CELLULAR BIOLOGY, Oct. 1997, p. 5813–5822 Vol. 17, No. 10
0270-7306/97/$04.00+0

Aberrant Silencing of the CpG Island-Containing Human O^6-Methylguanine DNA Methyltransferase Gene Is Associated with the Loss of Nucleosome-Like Positioning

SONAL A. PATEL, DAWN M. GRAUNKE, AND RUSSELL O. PIEPER*

Program in Molecular Biology and Division of Hematology/Oncology, Loyola University Chicago, Maywood, Illinois 60153

Received 5 March 1997/Returned for modification 17 April 1997/Accepted 1 July 1997

Tumor-associated aberrant silencing of CpG island-containing genes has been correlated with increased cytosine methylation, a "closed" chromatin structure, and exclusion of transcription factor binding in the CpG island/promoter regions of affected genes. Given the lack of understanding of what constitutes a closed chromatin structure in CpG islands, however, it has been difficult to assess the relationship among cytosine methylation, chromatin structure, and inappropriate gene silencing. In this study, nuclease accessibility analysis was used to more clearly define the chromatin structure in the CpG island of the human O^6-methylguanine DNA methyltransferase (MGMT) gene. Chromatin structure was then related to in vivo DNA-protein interactions and cytosine methylation status of the MGMT CpG island in human glioma cells varying in MGMT expression. The results of these studies indicated that the "open" chromatin structure associated with the MGMT CpG island in $MGMT^+$ cells consisted of an approximately 250-bp transcription factor-binding, nuclease-accessible, nucleosome-free region of DNA, whose formation was associated with at least four flanking, precisely positioned nucleosome-like structures. In $MGMT^-$ cells, this precise nucleosomal array was lost and was replaced by randomly positioned nucleosomes (i.e., the closed chromatin structure), regardless of whether methylation of the CpG island was spread over the entire island or limited to regions outside the transcription factor binding region. These results suggest that CpG islands facilitate the expression of housekeeping genes by facilitating nucleosomal positioning and that the conditions that alter the formation of this array (such as perhaps methylation) may indirectly affect CpG island-containing gene expression.

Normal human cells express approximately 100,000 different genes, many of which are expressed in a non-tissue-specific fashion (1, 21). The expression of these so-called housekeeping genes is commonly controlled by 5′ regulatory regions known as CpG islands. CpG islands are 500- to 2,000-bp sequences that, unlike the rest of the genome, are GC rich, enriched in the CpG dinucleotide, and devoid of cytosine methylation (10). Although CpG island-containing housekeeping genes are in general constitutively expressed, the regulation of expression of these genes has taken on an increased significance with the discovery that normally constitutively expressed CpG island-containing housekeeping genes can be randomly silenced in tumor cells (16, 22, 44). While in many cases the silencing of critical genes is likely to be fatal to a tumor cell, the silencing of select constitutively expressed genes may provide tumors with capabilities (enhanced growth or metastatic potential, drug resistance) that ultimately favor tumor progression. Therefore, the process by which tumor cells use aberrant gene silencing to "experiment" with their pattern of gene expression is of extreme importance to cancer biology and cancer chemotherapy.

Our studies concerning tumor-associated aberrant gene silencing have focused on the human, non-X-linked, CpG island-containing gene encoding O^6-methylguanine-DNA methyltransferase (MGMT). MGMT is a DNA repair protein that removes methyl and alkyl groups from the O-6 position of guanine in DNA. This simple one-step repair process is present in nearly all normal human tissues and protects normal cells from mutagenicity associated with O^6-methylguanine mispairing during DNA replication. A significant percentage of primary tumors and tumor cell lines, however, do not express MGMT. In these $MGMT^-$ cells, MGMT gene silencing, rather than conferring an advantage, enhances the cytotoxic potential of chemotherapeutic chloroethylnitrosoureas, DNA interstrand-cross-linking agents whose cytotoxicity is dependent on adduction of DNA at the O-6 position of guanine (8). Given that the 5′ regulatory region of the human MGMT gene is embedded in a CpG island (13), study of the aberrant tumor-associated silencing of the MGMT gene may not only contribute to the development of tumor-selective chloroethylnitrosourea-sensitizing strategies but may also serve as a model for understanding the process by which CpG island-containing genes as a whole are inappropriately silenced.

The process by which tumor cells silence the CpG island-containing MGMT gene, as well as other CpG island-containing genes, appears to involve an interplay among cytosine methylation, transcription factor binding, and chromatin structure. The association of cytosine methylation with CpG island-containing gene silencing has clearly been demonstrated in primary and cultured tumor cells in which the normally unmethylated CpG islands of expressed genes (including MGMT) have been shown to be methylated in the nonexpressed setting (5, 14, 37). The spatial relationship between methylation of CpG islands and gene silencing, however, remains unclear. Many CpG islands of silenced housekeeping genes appear to be methylated throughout the island (2, 19, 20, 35). Therefore, it has been suggested that methylation of transcription factor binding sites directly blocks transcription factor binding or that methylation of CpG islands may allow for interaction of the

* Corresponding author. Mailing address: Department of Medicine, Division of Hematology/Oncology, Loyola University Medical Center, Building 112, Room 328, 2160 South First Ave., Maywood, IL 60153. Phone: (708) 327-3141. Fax: (708) 327-3342. E-mail: rpieper@luc.edu.

DNA with non-sequence-specific methylated-DNA binding proteins, which in turn block transcription factor accessibility (27, 28). In several MGMT$^-$ cell lines, however, methylation of the CpG island is noted in regions surrounding the transcription factor binding sites but not in the transcription factor binding region itself (35, 36). Additionally, an MGMT$^+$ cell line (T98G) and its MGMT$^-$ subline (T98Gs), in which differences in methylation of the MGMT CpG island noted were very small and limited to regions surrounding the transcription factor binding area, have been described (35). It has been suggested that rather than having a direct effect on transcription factor binding, methylation of CpG islands at sites distant from the transcription factor binding area may influence transcription factor binding by influencing chromatin structure (17, 37). The relationship between methylation and chromatin structure, however, also remains unclear. The unmethylated CpG islands of expressed housekeeping genes display regions of nuclease hypersensitivity (23, 39) and take on what has been referred to as an "open" chromatin structure (6), while the variably methylated CpG islands of silenced housekeeping genes are inaccessible to exogenous nucleases and probably also to endogenous transcription factors (6). These observations have led to the suggestion that the silencing mechanism associated with CpG island-containing genes including MGMT appears to involve methylation-associated loss of open chromatin structure and exclusion of transcription factor binding (6). Given the lack of understanding of what constitutes open and closed chromatin structures in the MGMT CpG island, however, it remains difficult to assess how methylation may or may not affect the process of chromatin formation.

In this study, we have examined and defined the chromatin structure of the MGMT CpG island in MGMT$^+$ and MGMT$^-$ human glioma cells and have related the chromatin structure to changes in methylation and MGMT expression. The results of these studies suggest that in MGMT$^+$ cells, the open chromatin structure described for the MGMT CpG island can more accurately be described as a small region of transcription factor binding, nucleosome-free DNA, whose formation is associated with at least four precisely positioned flanking nucleosome-like structures. In MGMT$^-$ cells, this precise nucleosome-like array is lost and is replaced by randomly positioned nucleosomes, regardless of whether methylation of the CpG island is spread over the entire island or limited to regions surrounding the transcription factor binding sites. These results suggest that CpG islands facilitate the expression of housekeeping genes by facilitating nucleosomal positioning and that the conditions that alter the formation of this array (such as perhaps methylation) may indirectly affect CpG island-containing gene expression.

MATERIALS AND METHODS

Cell culture. The glioma cell lines used in this study were established from grade III or IV human astrocytomas and glioblastomas. The SF767 (Brain Tumor Research Center, University of California, San Francisco, Calif.) and U138 (American Type Culture Collection, Rockville, Md.) glioma cell lines were previously characterized as MGMT$^+$, while the A1235 and CLA (L. Erickson, Indiana University Medical Center, Indianapolis, Ind.) cell lines were previously characterized as MGMT$^-$ (5). The MGMT$^-$ T98Gs subline arose spontaneously from the MGMT$^+$ T98G glioma line, as previously described (35), and is phenotypically indistinguishable from the T98G line. Peripheral blood mononuclear cells were isolated from a healthy individual and collected by centrifugation through a Ficoll gradient as specified by the manufacturer (Organon Teknika Cappel, Durham, N.C.). T cells (MGMT$^+$) were separated from peripheral blood mononuclear cells with polyclonal immunoglobulin G-conjugated immunoselective beads (Biotecx Lab, Houston, Tex.). This separation yielded 10^5 T cells/ml of blood. The MGMT status of all cells and cell lines was verified before the beginning of this study.

Genomic library screening, cloning, and sequencing. A human lung fibroblast cell line (WI38) genomic library was screened as previously described (5) with a uniformly ^{32}P-radiolabeled DNA fragment of the MGMT CpG island from nucleotides (nt) 676 to 967 (in the MGMT promoter numbering system described in reference 13). Following hybridization, the filters were washed first with 2× SSPE (1× SSPE is 0.18 M NaCl, 10 mM NaH_2PO_4, and 1 mM EDTA [pH 7.7])–0.1% sodium dodecyl sulfate (SDS) for 15 min at room temperature and then with 0.1× SSPE–0.1% SDS at 58°C for 5.5 min in a Disc-Wisk washing system (Schleicher and Schuell, Keene, N.H.). Following primary, secondary, and tertiary screening of 10^6 plaques, six positive clones were identified. Phage DNA was isolated from these clones (Wizard Lambda DNA purification system; Promega, Madison, Wis.) and was digested with *Bam*HI alone (which cleaves the MGMT CpG island at nt 1) or in combination with enzymes known not to cleave within the published MGMT promoter sequence (13). Southern blot analysis of the products of these digestions with the same probe used for the library screening identified three positive clones.

A *Bam*HI fragment containing the region from nt 1 to 6000 was isolated from one of the three positive clones and was subcloned into the *Bam*HI site of pGEM-7Zf(−) (Promega) to create p6MGMT. The 6-kb *Bam*HI insert was further mapped for restriction enzyme recognition sequences, and an 1,800-bp *Sph*I fragment containing the previously published MGMT promoter sequence (13) was isolated and inserted in both orientations into the *Sph*I site of pGEM-7Zf (−) to create p1.8MGMT$^+$ and p1.8MGMT$^-$. Following isolation of single-stranded DNA (pGEM single strand system; Promega), dideoxy sequencing was performed with the Taq Track sequencing system (Promega). The primers used to determine the sequence of the nontranscribed strand were as follows: nt 1158 to 1210, primer 5′-CCGCGCCCCTAGAACGCTTTGCGTC-3′; nt 1210 to 1320, primer 5′-GGCAGCCTCGAGTGGTCCT-3′; and nt 1320 to 1430, primer 5′-GTGTTGCCCAGCCTTTCCC-3′. To sequence the transcribed strand, the primers used were as follows: nt 1430 to 1310, primer 5′-CGGAGGGAAAGCTGG CAG-3′; and nt 1310 to 1158, primer 5′-ACGCCAGTCCACAGTCAC-3′.

LMPCR analysis of in vivo DNA-protein interactions. SF767, U138, CLA, and A1235 cultured cells, as well as human T cells, were analyzed for in vivo DNA-protein interactions at nt 1 to 1190 of the MGMT CpG island by ligand-mediated PCR (LMPCR) under previously described conditions (6). LMPCR-suitable DNA devoid of DNA-protein interactions was generated as previously described (25, 38, 42). The sets of nested primers used in the analysis of the transcribed strand of the MGMT CpG island were as follows: nt 60 to 282, 5′-GCTCCCTCT GAAGGCTCCAG-3′ (LMP19), 5′-GAGTGTCCTCTGCTCCCTC CGAAG-3′ (LMP20), and 5′-GAGTGTCCTCTGCTCCCTCCGAAGGCTC-3′ (LMP21); nt 282 to 487, 5′-GTGAGGTACTGGGAGTTAGGAC-3′ (LMP22), 5′-CAAC ATAGCTTCTCTGGTGGACACAA-3′ (LMP23), and 5′-CAACATAGCTTCT CTGGTGGACACAATTC-3′ (LMP24); nt 480 to 801, 5′-TGCCCCCACGGCC CCCTGACA-3′ (LMP13), 5′-TCTCTGCTGGTCTGGGGGTCCCTGA-3′ (LMP14), and 5′-TCTCTGCTGGTCTGGGGGTCCCTGACTAG-3′ (LMP15); nt 703 to 864, 5′-CGGCCCATTTGGCAAACTAAG-3′ (LMP1), 5′-AGGCAC AGACCTCAGGCGGAAGCT-3′ (LMP2), and 5′-AGGCACAGACCTCAGG CGGAAGCTGGGA-3′ (LMP3); nt 864 to 1075, 5′-GATGCGCAGACTGCCT CAG-3′ (LMP4), 5′-TGGGCATGCGCCGACCCGGTC-3′ (LMP5), and 5′-TG GGCATGCGCCGACCCGGTCGGG-3′ (LMP6); and nt 1076 to 1190, 5′-CCC GGATATGCTGGGACAGC-3′ (LMP7), 5′-CCGCGCCCCTGAACGCTTTG CGTC-3′ (LMP8), and 5′-CCGCGCCCCTGAACGCTTTGCGTCCCGA-3′ (LMP9). To analyze the nontranscribed strand, the following primer sets were used: nt 1190 to 1090, 5′-CCTACCCACCCCCAGTCC-3′ (LMP34), 5′-CCGG GGGGTGGGCTGCCGCTT-3′ (LMP35), and 5′-CCGGGGGGTGGGCTGC CGCTTCACTC-3′ (LMP36); nt 1090 to 980, 5′-AGGGCGCCTGCAGGACCA CTC-3′ (LMP43), 5′-GGCTGCCACCGTCCCGAGGGAGA-3′ (LMP44), and 5′-GGCTGCCACCGTCCCGAGGGAGAGCTC-3′ (LMP45); nt 980 to 681, 5′-ACCGCCGCACCCCGCCCCAG-3′ (LMP16), 5′-ATCTCGCCCCGCCTCGG CTCCTG-3′ (LMP17), and 5′-ATCTCGCCCCGCCTCGGCTCCTGGACT-3′ (LMP18); nt 717 to 495, 5′-GGCGACGGGACACGCGGACTG-3′ (LMP10), 5′-GGCCTACCGGGAAGCCGGCCA-3′ (LMP11), and 5′-GGCCTACCGGG AAGCCGGCCATGTTC-3′ (LMP12); nt 495 to 237, 5′-TCACTCTTAGGGCC AGGACGA-3′ (LMP25), 5′-TGCGACTCGGGCCTCGCGCTCAG-3′ (LMP26), and 5′-TG CGACTCGGGCCTCGCGCTCAGAGAG-3′ (LMP27); and nt 237 to 1, 5′-CACACCTGCAATAATCCTCAAC-3′ (LMP28), 5′-GTGGTCTCTTC GATACAACCTCAG-3′ (LMP29), and 5′-GTGGTCTCTTCGATACAACCTC AGGATTG-3′ (LMP30).

Restriction enzyme accessibility assays. Nuclei from SF767, T98G, T98Gs, and CLA cells (the equivalent of 200 μg of DNA per cell line) were isolated as previously described (35) and incubated for 10 min at 37°C with 5 to 200 U of *Msp*I or 16 U of *Ava*II. Following lysis of the nuclei, the DNA was isolated and cleaved with *Eco*RI (5 U/μg of DNA) for 3 h at 37°C to decrease viscosity. *Msp*I- or *Ava*II-cleaved products from the MGMT CpG island were amplified by LMPCR under conditions identical to those described previously (6).

Lysolecithin-mediated permeabilization of glioma cells. SF767, T98G, T98Gs, and CLA cells were permeabilized by exposure to lysolecithin by a modification of the previously described procedure (30). Cells (the equivalent of 1,500 μg of DNA per cell line) were harvested by trypsinization, washed twice in cold lysolecithin buffer (150 mM sucrose, 80 mM KCl, 35 mM HEPES [pH 7.4], 5 mM KH_2PO_4–K_2HPO_4, 5 mM $MgCl_2$, 0.5 mM $CaCl_2$), and resuspended in 5 ml of lysolecithin buffer containing 0.5 mg of lysophosphatidylcholine (lysolecithin; Sigma) per ml. Following a 1-min incubation on ice, the cells were collected by centrifugation (4 s at 12,000 × *g*), washed twice in lysolecithin buffer at room

temperature, and resuspended in either RSB buffer (10 mM Tris [pH 8], 10 mM NaCl, 3 mM $MgCl_2$) at room temperature for DNase I digestions or MN buffer (50 mM Tris [pH 7.4], 60 mM KCl, 3 mM $CaCl_2$, 0.34 M sucrose) at room temperature for micrococcal nuclease (MNase) digestions. Permeabilization of cells was verified by incubation of lysolecithin-treated cells with trypan blue (0.2% in Hanks balanced salt solution) for 5 min. In all cases, more than 95% of cells remained structurally intact but did not exclude trypan blue.

DNase I and MNase hypersensitivity assays. Lysolecithin-permeabilized SF767, T98G, T98Gs, or CLA cells (the equivalent of 200 μg of DNA per cell line per treatment group) were resuspended in 100 μl of RSB or MN buffer and exposed to 0.1 to 100 U of DNase I or 0.001 to 1 U of MNase at 37°C for 10 min. The cells were lysed by the addition of 900 μl of solution C plus proteinase K (20 mM Tris [pH 8.0], 20 mM NaCl, 20 mM EDTA, 1% SDS, 600 μg of proteinase K per ml). After a 3-h incubation at 37°C, RNase A (100 μg/ml; Sigma Chemical Co., St. Louis, Mo.) was added, and the incubation was continued for an additional 1 h. Following phenol-chloroform extraction and ethanol precipitation, the DNA was quantitated and analyzed for size by gel electrophoresis. DNA samples of an appropriate size range were further cleaved with *Bam*HI (5 U/μg) at 37°C for 14 h. The DNA was then size fractionated in a 20- by 25-cm 1.2% agarose gel (model H4 electrophoresis system [Bethesda Research Laboratories]) at 40 V for 12 to 20 h in 1× TAE (40 mM Tris-acetate, 1 mM EDTA) (20 μg/lane), transferred to a nylon membrane, and hybridized to a ^{32}P-radiolabeled MGMT promoter probe spanning nt 1 to 412. The membrane was washed as previously described (34) and exposed to X-ray film. The results were visualized by autoradiography.

Generation of probes for library screening and for DNase I and MNase hypersensitivity assays. The fragment of the MGMT CpG island (nt 676 to 967) used to screen the genomic library was generated by PCR amplification with genomic DNA from human 8226/S myeloma cells as a template. PCR was performed with 1 μg of *Eco*RI-digested DNA in a reaction mixture composed of 1× PCR buffer (10 mM Tris [pH 8.3], 50 mM KCl, 1.5 mM $MgCl_2$); 100 μM each dATP, dCTP, and TTP; 75 μM 7′-deaza-2′-dGTP; 25 μM dGTP; 2.5 U of *Taq* polymerase; and 50 pmol each of primers corresponding to nt 676 to 696 and nt 949 to 967. The PCR parameters were as follows: initial denaturation for 5 min at 95°C; 35 cycles of 95°C for 1 min, 62°C for 15 s, and 72°C for 15 s; and a final extension for 5 min at 72°C. The resultant PCR product was ligated into pCR II (Invitrogen, San Diego, Calif.), and the ligation products were used to transform *Escherichia coli* INV F″ cells (Invitrogen). Individual colonies were isolated and analyzed for the presence of the appropriate-size insert. The identity of the MGMT CpG island insert was confirmed by dideoxy sequencing.

The MGMT CpG island fragment (nt 1 to 412) used as a probe in the DNase I and MNase hypersensitivity assays was generated by cleavage of p6MGMT with *Bam*HI and *Bgl*I (10 U/μg of DNA) at 37°C for 1 h. Following size fractionation of the products in a 2% agarose gel (SeaPlaque GTG; FMC, Rockland, Maine), the *Bam*HI-*Bgl*I fragment of approximately 420 bp was excised from the gel and purified by centrifugation (13,000 × *g* for 1 min) through glass wool. The probe was labeled by the random-primer method with [α-^{32}P]dCTP (3,000 Ci/mmol; Amersham) (9). The specific activity of the probe was $>1.0 \times 10^9$ cpm/μg.

The 100-bp ladder was radiolabeled by the phosphate exchange reaction as specified by the manufacturer (Bethesda Research Laboratories).

Nucleotide sequence accession number. The MGMT CpG island sequence (nt 480 to 1250) has been submitted to GenBank and assigned accession no. U95038.

RESULTS

Cloning of the MGMT CpG island. A complete assessment of the chromatin structure of the MGMT CpG island required the complete DNA sequence of the region. To obtain this sequence, a PCR-generated probe based on a published partial sequence of the MGMT CpG island was used to screen a genomic library derived from normal human fibroblasts. After primary, secondary, and tertiary screening, a clone containing all of the published MGMT CpG island sequence as well as 17 kb of additional sequence was recovered. Partial sequencing of the insert in this clone and the subsequent CpG dinucleotide distribution analysis of the sequence revealed that the MGMT CpG island spanned nt 480 to 1250.

Identification of DNA-protein interactions in the MGMT CpG island. To understand the chromatin structure of the MGMT CpG island and to ultimately relate the chromatin structure of the MGMT CpG island to MGMT expression, a complete analysis of DNA-protein interactions in the MGMT CpG island in MGMT$^+$ and MGMT$^-$ cells was required. Previous analysis of in vivo DNA-protein interactions in a limited region of the MGMT CpG island identified seven sites of DNA protein interactions which occurred exclusively in MGMT$^+$ cells (6). Six of these interactions were at consensus Sp1 binding sites, and the seventh was at a previously unidentified site. To extend this analysis to the rest of the MGMT CpG island, 12 LMPCR primer sets were generated and used in in vivo footprint analysis of both strands of the MGMT CpG island in a variety of MGMT$^+$ and MGMT$^-$ cells. DNA from dimethyl sulfate (DMS)-treated cells was isolated, cleaved at adducted guanines with piperidine, and amplified with MGMT CpG island-specific primers. DNA-protein interactions were identified by comparing the LMPCR products generated by using DNA which was potentially protein bound at the time of DMS exposure with those generated by using DNA devoid of DNA-protein interactions ("naked" DNA) at the time of DMS exposure. Consistent with the previous analysis, seven sites of DNA-protein interactions were noted in the region between nt 850 and 1020. These interactions, as before, were noted only in MGMT$^+$ SF767 glioma cells and human T cells but not in MGMT$^-$ CLA or A1235 cells (Table 1). Additional LMPCR analysis of both strands of the MGMT CpG island region nt 1 to 850 and nt 1020 to 1190 revealed no evidence of either proected regions or hypersensitive guanines in comparing banding patterns generated by using "naked" DNA with those generated by using DNA from DMS-treated MGMT$^+$ or MGMT$^-$ cells (Table 1). Based on these results, sequence-specific DNA-protein interactions in the MGMT CpG island appear to be limited to a 200-bp region of the island in MGMT$^+$ cells, as shown in Fig. 1.

TABLE 1. DNA-protein interactions in the 5′ region of the MGMT gene as detected in MGMT$^+$ SF767 and MGMT$^-$ A1235 glioma cells and in normal human T cells

Region analyzed (nt)	Strand analyzed	DNA-protein interaction(s) in:	
		SF767 and T cells	A1235 cells
60–282	Transcribed	None	None
282–487	Transcribed	None	None[a]
480–801	Transcribed	None	None
702–864	Transcribed	Novel protein	None
864–1075	Transcribed	6 Sp1-like proteins	None[a]
1076–1190	Transcribed	None[b]	None[a]
1190–1090	Nontranscribed	None[b]	None[a]
1090–980	Nontranscribed	None	None[a]
980–681	Nontranscribed	Novel protein	None[a]
717–495	Nontranscribed	None	None
495–237	Nontranscribed	None	None[a]
237–0	Nontranscribed	None	None[a]

[a] Additionally analyzed in MGMT$^-$ CLA cells.
[b] Additionally analyzed in MGMT$^+$ U138 cells.

Restriction endonuclease accessibility in the MGMT CpG island. Previous analysis of a small region of the MGMT CpG island (nt 712 to 1028) suggested that Sp1-like interactions in MGMT$^+$ cells were associated with a region of open chromatin structure that was unmethylated and accessible to restriction enzyme cleavage (data summarized in Fig. 1) (6). Lack of DNA-protein interactions in MGMT$^-$ cells was associated with a closed chromatin structure in a region of DNA that was in some cases methylated and in other cases unmethylated but in all cases inaccessible to restriction enzyme cleavage. To better understand the basis for open and closed chromatin structure and to potentially relate chromatin structure to DNA methylation and to known sites of DNA-protein interaction, the analysis of restriction enzyme accessibility was expanded to include the entire MGMT CpG island. In these experiments, nuclei from cells were incubated with various amounts of the

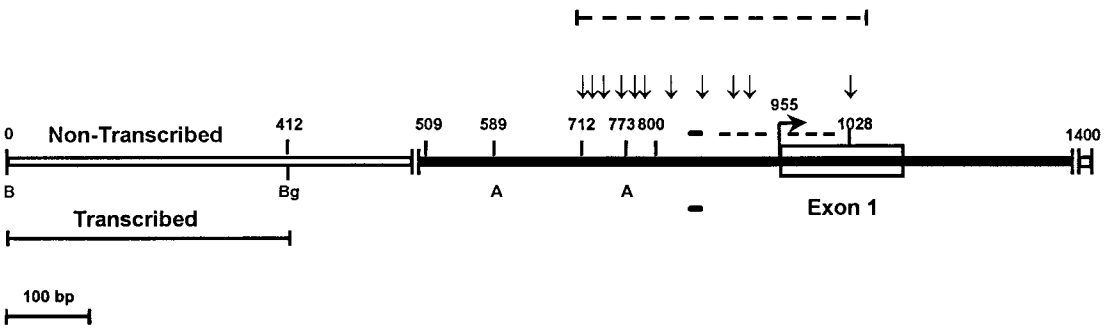

FIG. 1. Transcription factor binding sites and previously identified sites of restriction enzyme accessibility in the MGMT CpG island. ⊢⊣, probe for DNase I and MNase hypersensitivity; −, Sp1-like binding site; **–**, novel binding site; ⊢----⊣, regions analyzed for accessibility; ↓, sites of enhanced accessibility in MGMT$^+$ cells; ▬, CpG island; ⌐→, transcription start site; B, *Bam*HI site; Bg, *Bgl*I site; A, *Ava*II site.

restriction enzyme *Msp*I or *Ava*II. The ability of these restriction enzymes to access and cleave the MGMT CpG island was reflected in the amount of LMPCR-amplified products generated with the in vivo restriction enzyme-cleaved DNA as template. The use of different restriction enzymes and different LMPCR primer sets allowed the analysis of the accessibility of nearly the entire MGMT CpG island. The MGMT$^+$ cell lines used for these analyses were SF767, which does not exhibit methylation of the MGMT CpG island, and T98G, which exhibits a small degree of methylation in regions surrounding the MGMT CpG island transcription factor binding region but not in the transcription factor binding region itself (35). The MGMT$^-$ cell lines used were T98Gs and CLA. T98Gs is a subline of T98G and, like T98G, exhibits little or no methylation of the transcription factor binding region of the MGMT CpG island. In the remaining regions of the island, however, T98Gs cells exhibit slightly higher levels of methylation than do T98G cells (35). CLA cells exhibit extensive methylation throughout the entire MGMT CpG island (35).

Incubation of nuclei from MGMT$^+$ SF767 and T98G cells with small amounts (5 or 20 U) of *Msp*I resulted in cleavage of the MGMT CpG island and the subsequent generation of PCR products visible in the autoradiograph presented in Fig. 2. In SF767 and T98G nuclei, the MGMT CpG island was preferentially cleaved in the region beginning at approximately nt 750 and was significantly less cleaved at *Msp*I sites in the region from nt 500 to 750 (e.g., nt 509, 539, 712 [Fig. 2, lanes 1 and 2 and lanes 5 and 6]). Exposure of equal amounts of MGMT$^+$ SF767 and T98G nuclei to higher *Msp*I concentrations (100 or 200 U) resulted in cleavage at all *Msp*I recognition sequences, demonstrating that all *Msp*I sites could be cleaved and could give rise to LMPCR products provided that the amount of *Msp*I used was sufficient to completely degrade the higher-order chromatin structure. The lack of larger LMPCR products corresponding to the *Msp*I sites at nt 856 and 917 in these samples (Fig. 2, lanes 3 and 4 and lanes 7 and 8) is the result of the amplification procedure. For LMPCR-based analysis of restriction enzyme accessibility, the *Msp*I-digested fragments are denatured and copied with (in Fig. 2) a primer complementary to nt 422 to 443 and oriented in the nt 509-to-917 direction. As a result, in completely or nearly completely digested samples, the number of fragments available for amplification decreases as the distance from the primer increases.

In contrast to the data for MGMT$^+$ cells, in MGMT$^-$ T98Gs and CLA nuclei, very little cleavage of any *Msp*I site was noted following incubation of the nuclei with 5 or 20 U of *Msp*I (Fig. 2, lanes 9 and 10 and lanes 13 and 14). Following exposure of T98Gs or CLA nuclei to 100 or 200 U of *Msp*I, however, all the *Msp*I sites could be cleaved, with the resultant pattern and intensity of amplification products similar to those generated with DNA from *Msp*I-digested MGMT$^+$ SF767 and T98G nuclei. A similar result was noted when SF767, T98G, T98Gs, or CLA nuclei were incubated with a fixed amount of *Ava*II. In MGMT$^+$ SF767 and T98G nuclei, the MGMT CpG island was digested, with the *Ava*II site at nt 773 being cleaved in preference to the site at nt 589 (Fig. 2, panel *Ava*II). In MGMT$^-$ T98Gs and CLA nuclei, the same amount of *Ava*II was insufficient to cleave any *Ava*II site. The pattern of *Msp*I

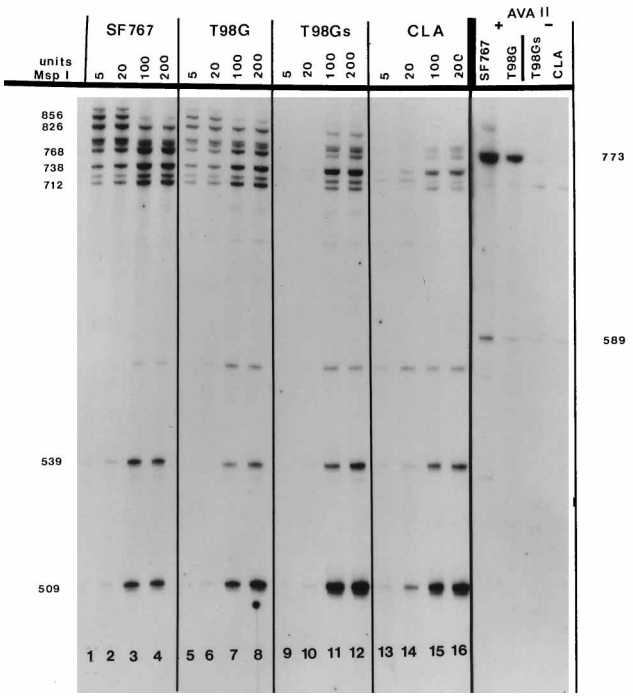

FIG. 2. LMPCR analysis of restriction enzyme accessibility to the MGMT CpG island at nt 509 to 856 within intact nuclei from MGMT$^+$ cells (SF767 and T98G) and MGMT$^-$ cells (T98Gs and CLA). Nuclei were incubated with 5 to 200 U of *Msp*I or 16 U of *Ava*II for 10 min at 37°C, the DNA was isolated, and 5 μg was analyzed by LMPCR with primers LMP14 and LMP15. Equal-volume aliquots of the reaction products were electrophoresed on a 6% denaturing polyacrylamide gel, after which the radiolabeled products were autoradiographed for 2 to 5 h. First four panels, *Msp*I accessibility; rightmost panel, *Ava*II accessibility. The autoradiograph is representative of four independent analyses.

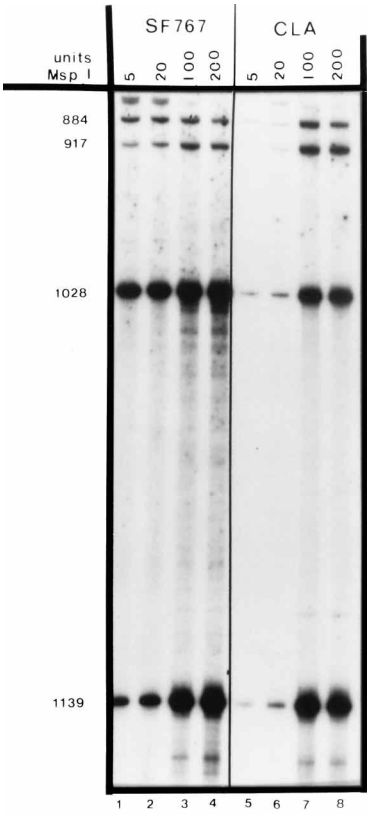

FIG. 3. LMPCR analysis of *Msp*I accessibility to the MGMT CpG island at nt 1139 to 884 within intact SF767 and CLA nuclei. The nuclei were incubated with *Msp*I, DNA was isolated, and LMPCR analysis was performed (with primers LMP34 to LMP36) as described in the legend to Fig. 2.

and *Ava*II cleavage noted in the MGMT CpG island of $MGMT^+$ and $MGMT^-$ cells was not due to variations in the methylation status of *Msp*I or *Ava*II recognition sequences, because *Msp*I cleavage is methylation independent and because none of the *Ava*II sites analyzed contained a CG dinucleotide. Rather, the variability in cleavage was probably due to the variability in the accessibility of the recognition sequence to the restriction enzyme, which was in turn a result of chromatin structure.

Extension of analysis of restriction enzyme accessibility to the MGMT CpG island region from nt 917 to 1139 suggested that, just as there was an abrupt increase in the nuclease accessibility of the MGMT CpG island in $MGMT^+$ cells between nt 600 and 750, there was also a relatively abrupt decrease in nuclease accessibility between nt 1028 and 1139. As seen in Fig. 3, the *Msp*I site at nt 1139 in the nuclei of $MGMT^+$ SF767 cells was somewhat accessible to cleavage by small amounts of *Msp*I, although the cleavage was, by autoradiographic analysis, approximately three times lower than that noted at the *Msp*I site at nt 1028 (Fig. 3, lanes 1 and 2). Based on the data from Fig. 2 and on previously published data (5), the *Msp*I sites at 917 nt and 884 probably also were accessible to cleavage by small amounts of *Msp*I. The lower signal intensity of bands corresponding to these sites in lanes 1 and 2 of Fig. 3 is again the result of the orientation of analysis (nt 1139 to 884); i.e., most DNA cleaved at 917 or nt 884 was also cleaved at either nt 1139 or 1028. Again, in the analysis presented in Fig. 3, increasing the amount of *Msp*I resulted in nonpreferential cleavage of all *Msp*I sites in both $MGMT^+$ and $MGMT^-$ cells and in equal cleavage of the *Msp*I sites at nt 1139 and 1028 in both cell types.

A final analysis of accessibility of the MGMT CpG island to MspI is presented in Fig. 4. Although it is not possible to directly compare to the banding intensity in Fig. 3, the *Msp*I site at nt 1139, which was only moderately sensitive to cleavage by small amounts of *Msp*I (Fig. 3), was more sensitive to cleavage by small amounts of *Msp*I than were (in decreasing degree of accessibility) the sites at nt 1245, 1301, and 1407. The reduced intensity of larger bands (i.e., nt 1245, 1301, and 1407) was not due to excessive cleavage at nt 1139, since the amount of larger products increased as increasing amounts of *Msp*I were used. The region at nt 1139 to 1407 remained more accessible to small amounts of *Msp*I in $MGMT^+$ cells than in $MGMT^-$ cells, although increased exposure of nuclei to *Msp*I increased the total amount of cleavage in a nonpreferential manner in both $MGMT^+$ and $MGMT^-$ cells and resulted in roughly equal cleavage of all sites in all cell groups.

As a whole, the results presented in Fig. 2 to 4 suggest that the MGMT CpG island in $MGMT^+$ cells contains a well-defined region of accessible DNA (approximately nt 600 to 1020) that is surrounded by regions of lesser accessibility. In contrast, the MGMT CpG island in $MGMT^-$ cells is uniformly less accessible to DNA-interactive proteins than is the MGMT CpG island in $MGMT^+$ cells.

Positioning of nucleosome-like structures in the MGMT CpG island of $MGMT^+$ and $MGMT^-$ cells. While restriction enzyme accessibility studies establish that a pattern of accessi-

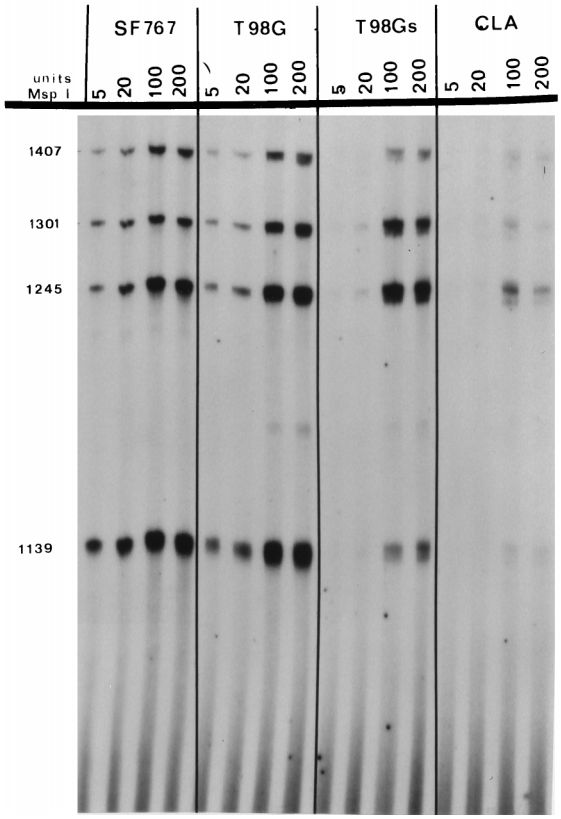

FIG. 4. LMPCR analysis of *Msp*I accessibility to the MGMT CpG island at nt 1139 to 1407 within intact nuclei from SF767, T98G, T98Gs, and CLA tumor cells. Nuclei were incubated with *Msp*I, DNA was isolated, and LMPCR analysis was performed (with primers LMP7 to LMP9) as described in the legend to Fig. 2.

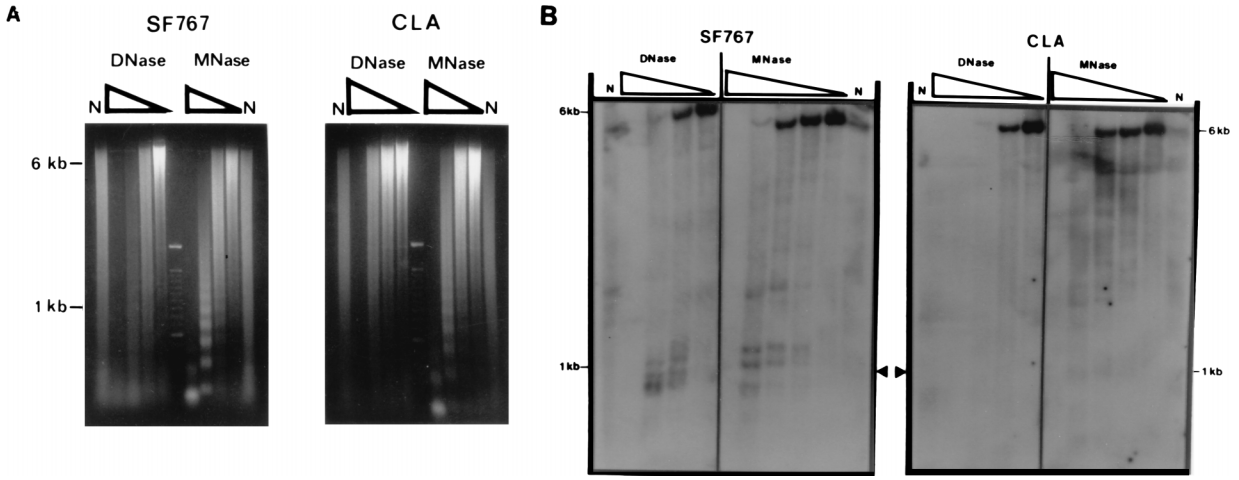

FIG. 5. Southern blot analysis of DNase I and MNase hypersensitivity in the MGMT CpG island. (A) Lysolecithin-permeabilized SF767 and CLA cells were exposed to DNase I (100, 10, 5, or 0.1 U) or MNase (1, 0.05, 0.01, 0.005, and 0.001 U) at 37°C for 10 min. The DNA was then isolated, cleaved with *Bam*HI, electrophoresed (20 μg/lane) in an ethidium bromide-containing 1.2% agarose gel next to a 100-bp ladder, transferred to a nylon membrane, and hybridized to a uniformly ^{32}P-radiolabeled *Bam*HI-*Bgl*I fragment (nt 1 to 412) of the MGMT promoter. (B) The membrane was then washed and exposed to X-ray film. Isolated genomic DNAs exposed to DNase I (0.005 U) or MNase (0.001 U) and handled in a manner similar to cellular DNA samples were also included in these studies (N lanes). The data are representative of three independent experiments. The arrowheads indicate nuclease-generated DNA fragments present in SF767 DNA but absent in CLA DNA.

bility exists in the MGMT CpG island, they do not explain this pattern. Previous suggestions that methylated-DNA binding proteins may block the accessibility of DNA-interactive proteins appear to be inconsistent with MGMT CpG island restriction enzyme accessibility data, since regions of the island which are inaccessible can exist in both methylated (as in MGMT$^-$ CLA cells) or unmethylated (as in MGMT$^-$ T98Gs or MGMT$^+$ SF767 cells) states. A second possible basis for the patterning of nuclease accessibility in the MGMT CpG island of MGMT$^+$ cells is nucleosomal positioning. To address the possibility that the nucleosome location dictates DNA accessibility, the positioning of nucleosome-like structures was analyzed. Lysolecithin-permeabilized MGMT$^+$ and MGMT$^-$ cells were incubated with various concentrations of DNase I or MNase, after which the DNA was isolated and subjected to Southern blot analysis. DNase I preferentially cleaves regions of double-stranded DNA which are devoid of nucleosomes (7) or in some cases DNA which is positioned between nucleosomes and transcription factor binding sites (40). MNase recognizes unpaired bases and preferentially cleaves DNA between nucleosomes and in regions of single-strand exposure (4, 7, 12). The sites of DNase I and MNase cleavage in the MGMT CpG island of MGMT$^+$ and MGMT$^-$ cells were assessed by digesting isolated DNase I- or MNase-cleaved DNA with *Bam*HI and hybridizing the electrophoresed DNA to an MGMT CpG island-specific probe generated from the end of the MGMT CpG island-containing *Bam*HI fragment (Fig. 1). In the absence of nuclease-hypersensitive sites, the probe would be expected to hybridize to a 6-kb *Bam*HI fragment. In instances in which the MGMT CpG island present within the *Bam*HI fragment contained sites of nuclease hypersensitivity, the probe would be expected to hybridize to smaller fragments, whose sizes would correspond to the distance between the nuclease-hypersensitive site and the end of the probe. The results of this type of experiment performed with DNA from lysolecithin-permeabilized MGMT$^+$ SF767 and MGMT$^-$ CLA cells incubated with various concentrations of DNase I or MNase are shown in Fig. 5. In the DNA from DNase I-digested SF767 cells, the probe recognized a 6-kb *Bam*HI fragment, as well as a series of discrete, DNase I-generated smaller bands, the most prominent being approximately 1 kb in size (left side of Fig. 5B). In DNA from MNase-digested SF767 cells, a similar series of DNA fragments was recognized by the probe, as were, to a lesser extent, both smaller (approximately 600-bp) and larger (approximately 1,500-bp) fragments. Identical fragments were noted in similarly DNase I- or MNase-digested T98G cells (data not shown). In the DNA from MGMT$^-$ CLA cells (and from T98Gs cells [data not shown]), no such DNase I or MNase hypersensitivity was apparent (right side of Fig. 5B), although the CLA DNA was digested to an equal extent by DNase I or MNase (as seen in the ethidium bromide-stained gel of the electrophoresed DNA prior to transfer [Fig. 5A]). The sites of nuclease hypersensitivity noted in SF767 cells were not a result of preferential DNA sequence-based cleavage, since no preferential DNA cleavage was noted in the MGMT CpG island of purified SF767 or CLA DNA (Fig. 5B, lanes N) digested to a similar degree with either DNase I or MNase. Rather, these sites of preferential nuclease cleavage were the result of the packaging of the DNA in the cells at the time of nuclease exposure. To better localize the regions of nuclease hypersensitivity in the MGMT CpG island of SF767 cells, DNA samples from cells exposed to DNase I (10 or 5 U [Fig. 5]) or MNase (0.05 or 0.01 U [Fig. 5]) were reelectrophoresed, and a more detailed Southern blot analysis was carried out. The results of these studies (Fig. 6) suggested a periodic distribution of nuclease hypersensitivity in the MGMT CpG island of MGMT$^+$ cells. As shown in Fig. 6, strongly DNase I-hypersensitive sites were noted near nt 850, which corresponds to the binding site of an unknown double-stranded DNA binding protein; at approximately nt 950, which corresponds to the MGMT transcription start site; and near nt 800 and 1020, which correspond to the edges of the nuclease-accessible region as defined by restriction enzyme accessibility analysis. A weaker site of DNase I cleavage was noted at approximately nt 600. Strong MNase-hypersensitive sites (Fig. 6) were located at approximately nt 800, 950, 1020, 1220, 1400, and 1580, with a weaker site at nt 600. This data, along with information from restriction enzyme accessibility studies and in vivo footprint analysis, is compiled in Fig. 7.

The most reasonable explanation of the periodic nuclease cleavage pattern noted in the MGMT CpG island of MGMT$^+$ cells is that the region between nt 800 and 1020 is

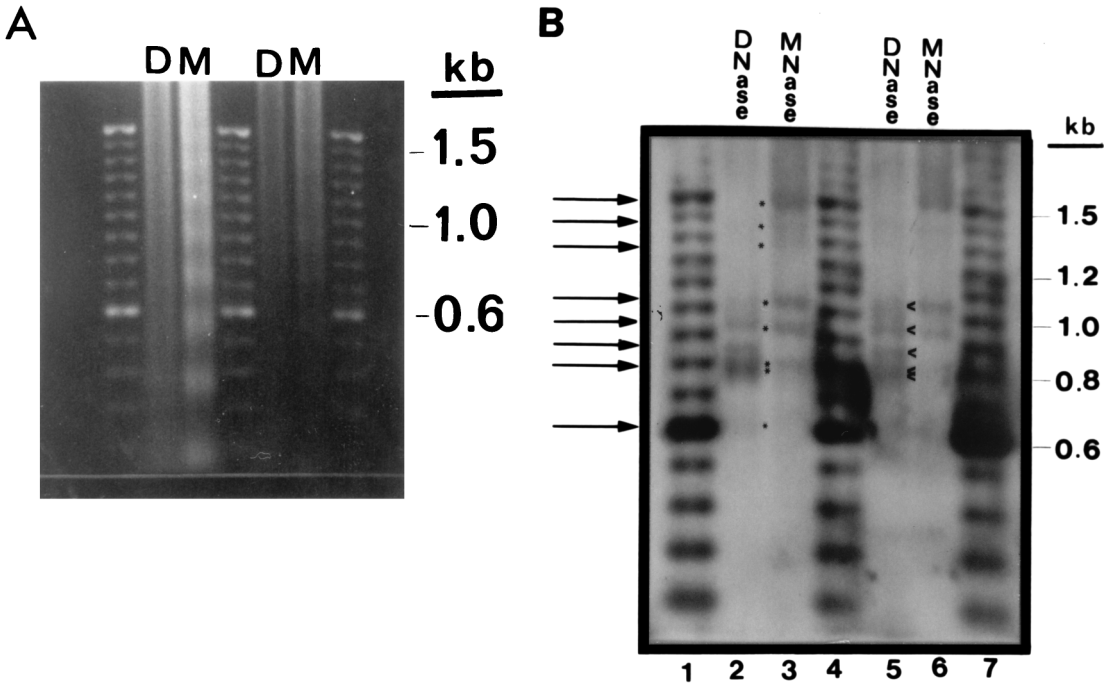

FIG. 6. Detailed Southern blot analysis of DNase I and MNase hypersensitivity in the MGMT CpG island of SF767 cells. (A) DNA samples generated by exposure of lysolecithin-permeabilized SF767 cells to DNase I (10 U [lane 2] or 5 U [lane 5]) or MNase (0.05 U [lane 3] or 0.01 U [lane 6]) were reelectrophoresed in an ethidium bromide-containing 1.2% gel next to a ^{32}P-end-labeled 100-bp ladder (20,000 cpm/lane). (B) The DNA was then transferred to a membrane and hybridized to a radiolabeled fragment of the MGMT promoter as described in Fig. 5, after which the membrane was washed and exposed to X-ray film. Arrowheads indicate sites of DNase I hypersensitivity; asterisks and arrows on the left indicate sites of MNase hypersensitivity. The data are representative of three independent experiments.

devoid of nucleosomes and is thus DNase I hypersensitive. The region of DNA near nt 950 is DNase I hypersensitive probably because it corresponds to the MGMT transcription start site (13) and as such is probably in a perpetually melted single-stranded state in MGMT$^+$ cells (43). The DNA region at approximately nt 850 may also be similarly distorted and nuclease hypersensitive as a result of its interaction in MGMT$^+$ cells with an unknown double-stranded DNA binding protein (6). Because MNase preferentially cleaves between nucleosomes and because nucleosomes occupy approximately 160 to 200 bp of DNA (39), the MNase digestion pattern is probably the result of MNase cleavage between nucleosomes or nucleosome-like structures positioned at nt 600 to 800, 1000 to 1200, 1200 to 1400, and 1400 to 1600 in a significant percentage of cells. Additional nucleosome-like structures may be present between nt 400 to 600 and nt 1600 to 1800 depending on the MNase sensitivity of the boundary between positioned and random nucleosomes. Since preferential cleavage of the MGMT CpG island is not noted in MGMT$^-$ cells, the data suggest that an array of positioned nucleosomes or nucleosome-like structures may not exist in such cells and that the MGMT CpG island in MGMT$^-$ cells may rather be associated with randomly positioned nucleosomes. As a whole, these data suggest the model presented in Fig. 8. In MGMT$^+$ cells, the MGMT CpG island is associated with at least four nucleosomes (with five nucleosomes depicted in Fig. 8) or nucleosome-like structures that are precisely positioned in the majority of cells. These structures render associated regions inaccessible to restriction enzymes (and transcription factors). The positioned nucleosome-like structures, however, appear to allow for (or perhaps are allowed by) a nucleosome-free gap in the island to which transcription factors bind and stimulate transcription. In MGMT$^-$ cells, this organization appears to be lost, so that no sites of nuclease hypersensitivity are apparent and, despite the presence of the appropriate transcription factors, no transcription factor binding is noted.

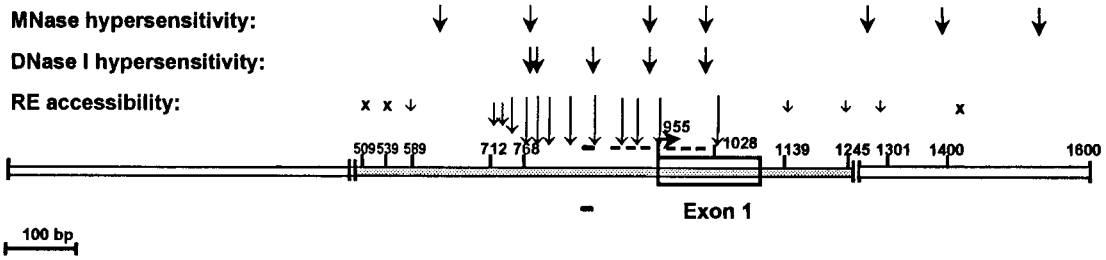

FIG. 7. Summary of restriction enzyme accessibility and nuclease hypersensitivity in the MGMT CpG island. For restriction enzyme (RE) accessibility, the sizes of the arrows are proportional to the degree of accessibility. ×, inaccessible sites; −, Sp1 site; ▬, novel binding site; ↓, sites of enhanced accessibility in MGMT$^+$ cells; ▭, CpG island; ⇾, transcription start site; ↓, sites of nuclease hypersensitivity in MGMT$^+$ cells.

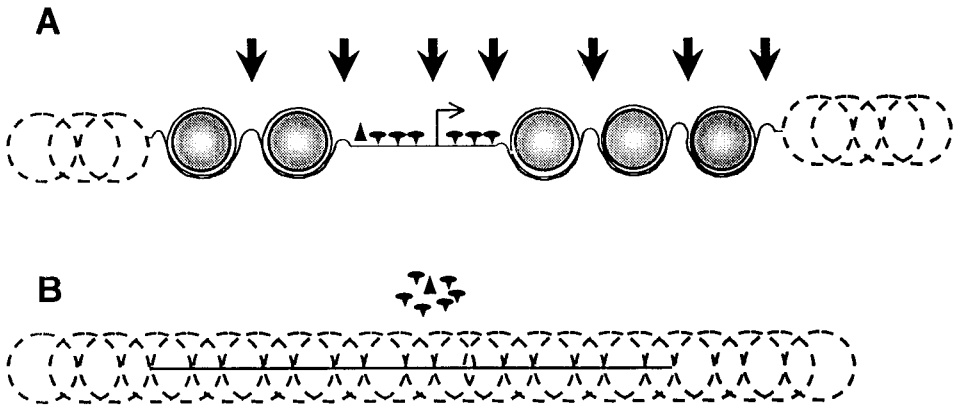

FIG. 8. Model for the aberrant silencing of the CpG island-containing human MGMT gene. (A) MGMT expression is associated with a nucleosome-free region of transcription factor binding that is surrounded by at least four (here depicted as five) positioned nucleosome-like structures (B) Tumor-associated MGMT silencing is associated with loss of nucleosome positioning and exclusion of transcription factor binding. ⌐→, transcription start site; ↓, MNase-hypersensitive sites; ▲, novel protein; 🔻, Sp1-like protein.

DISCUSSION

The data presented in this paper suggest that the expression of the human, non-X-linked CpG island-containing MGMT gene is associated with a precise chromatin structure involving the positioning of nucleosome-like structures. The data are internally consistent as well as being consistent with published information about CpG islands. With regard to internal consistency, regions of the MGMT CpG island that do not interact with DNA binding proteins, as assessed by in vivo footprint analysis, are also inaccessible to interactions with nucleases (restriction enzymes, DNase I). In contrast, regions that interact with transcription factors are also accessible to other DNA-interactive proteins (restriction enzymes, DNase I). Regions of DNA in the MGMT CpG island of $MGMT^+$ cells that are cleaved by MNase either are located at the edge of regions associated with transcription factors, at the transcription start site, or are spaced at nucleosome-sized intervals in regions of nuclease inaccessibility. As such, the exact positioning of nucleosome-like structures around a nonnucleosomal, transcription factor binding, nuclease-accessible region appears to be the best explanation of the data presented. The possibility that the MNase digestion pattern was created by non-histone DNA binding proteins, while not formally excluded, is less likely, given the repeated nature of the structures observed and the lack of in vivo DNA-protein interactions in the areas proposed to be associated with nucleosome-like structures (histones, unlike sequence-specific DNA binding proteins, do not protect DNA from DMS-induced damage [33]). As well as being internally consistent, the data are consistent with the observation that CpG islands frequently contain 60- to 300-bp regions of nonnucleosomal DNA (39). Finally, the data are strikingly similar to those noted in the CpG island-containing mouse X-linked APRT gene, in which a slightly altered positioning of nucleosomes has been suggested (23).

The present data, in addition to suggesting a model for normal chromatin structure in expressed CpG islands, suggest that the inactivation of the CpG island-containing MGMT gene involves alteration of normal chromatin structure. While the data from $MGMT^+$ cells are suggestive of nucleosomal positioning, the data concerning the MGMT CpG island in $MGMT^-$ cells could be interpreted in a number of different ways. It is possible that the aberrant silencing of the MGMT gene is associated not with dramatic changes in chromatin structure but merely with the positioning of a nucleosome in the transcription factor binding region of the MGMT CpG island. Support for this mechanism comes from studies suggesting that silencing of the X-linked HPRT gene is associated with extensive methylation of its 5′ CpG island and the positioning of one or two nucleosomes in a normally nucleosome-free, transcription factor binding region of the island (32). The nucleosome-free gap in the MGMT CpG island of $MGMT^+$ cells is of the appropriate size to accommodate a nucleosome, and the positioning of such a nucleosome would be expected to block both transcription factor binding and gene expression. Such nucleosomal positioning would, however, be expected to produce MNase- and perhaps DNase I-hypersensitive sites in $MGMT^-$ cells. Because such nuclease hypersensitive sites are not noted in this or any other regions in the MGMT CpG island of $MGMT^-$ cells, the silencing mechanism associated with the X-linked human HPRT gene appears to differ from that noted in the autosomal MGMT gene. A second possible interpretation of the data from $MGMT^-$ cells is that the lack of transcription factor binding and nuclease accessibility throughout the MGMT CpG island is the result of the binding of non-sequence-specific methylated-DNA binding proteins. At least two such proteins, MeCP1 and MeCP2, have been identified, and their binding could be supposed to exclude transcription factors as well as exogenous nucleases (27, 28). This scenario appears to be inconsistent with MGMT silencing in the T98Gs cells, in which the entire CpG island is inaccessible to nucleases and transcription factors while the region corresponding to the transcription factor binding region is devoid of methylation (35). MeCP2 can, however, bind DNA containing even a single symmetrically methylated CpG dinucleotide (30), and very low levels of methylation in the MGMT CpG island of T98Gs cells could escape detection by the methods used for analysis. If involved, the binding of such proteins would, in addition to directly excluding transcription factor binding, be required to indirectly alter nucleosome-like positioning, since no DNase I- or MNase-hypersensitive sites were noted in the MGMT CpG island of $MGMT^-$ cells. Additionally, if methylated-DNA binding proteins do bind and influence chromatin structure, they must bind very weakly or transiently, since there was no evidence of these proteins in in vivo footprint analysis of the methylated MGMT CpG island of $MGMT^-$ CLA cells. Nonetheless, the possibility that methylated-DNA binding proteins play a role in MGMT silencing cannot be rigorously excluded. A third scenario, however, which appears to be most

consistent with the present data, is that the precise nucleosome-like array suggested by analysis of the MGMT CpG island in $MGMT^+$ cells is lost in $MGMT^-$ cells and is replaced by randomly positioned nucleosomes. These randomly positioned nucleosomes do not allow for the creation of nuclease-hypersensitive sites and probably also do not allow for any given cell to contain all the transcription factor-DNA interactions necessary for MGMT expression.

The positioning of nucleosome-like structures in the MGMT CpG island in $MGMT^+$ cells and the loss of this precise chromatin structure in $MGMT^-$ cells has a significant impact on how the process of aberrant silencing of CpG island-containing genes can be viewed. Transcription factor binding regions in CpG islands are important in gene expression, and alterations in methylation and/or chromatin structure of these regions probably directly affect gene expression. If, however, the establishment of nucleosome-free, transcription factor binding regions in CpG islands is associated with exact positioning of nucleosome-like structures in the non-transcription factor binding regions of CpG islands, changes in methylation or chromatin structure outside the transcription factor binding area may significantly influence CpG island-containing gene expression. The issue of how methylation can influence distant chromatin structure has recently been addressed by Kass et al. (18). In that study, methylation of plasmid regions surrounding a microinjected herpes simplex virus thymidine kinase gene directed a time-dependent, chromatin-associated repression of transcription initiation. The linkage between methylation, nucleosome assembly, and gene silencing noted by Kass et al. bears strong similarities to the data in the present study, although in the case of the silenced MGMT CpG island, the methylation-associated changes in chromatin structure appear to be associated not with specific nucleosomal positioning over transcription factor binding regions but, rather, with a generalized loss of precise nucleosomal positioning. In addition to the above-cited studies, there is evidence to suggest that nucleosome assembly is influenced, both positively and negatively, by methylation (11) and that histone H1, by virtue of preferential binding to methylated DNA, is involved in the stabilization of higher-order chromatin structure and transcriptional repression (26). As a whole, these studies suggest linkage at a distance among methylation, nucleosome formation, and gene silencing. Such a linkage is supported by the observation that in some silenced CpG islands, methylation occurs only in regions outside the transcription factor binding region and not in the transcription factor binding region itself (35, 36, 41). Additionally, since the processes of chromatin disassembly/reassembly and methylation both occur near the replication fork following each S phase (15), both physical and temporal linkage may be possible. Even if one assumes that the positioning of nucleosomes allows for transcription factor binding and not vice versa, the direct linkage among methylation, chromatin structure, and gene expression may not be absolute. As noted, the $MGMT^+$ T98G and $MGMT^-$ T98Gs cell lines both exhibit a slight degree of methylation of the MGMT CpG island in regions outside the transcription factor binding area yet differ dramatically in the MGMT expression and nuclease accessibility of these areas (35). Therefore, either very small changes in methylation in CpG islands can trigger loss of nucleosomal positioning, or factors other than methylation can influence the likelihood of formation of a precise chromatin structure. The identification of such an ordered chromatin structure in $MGMT^+$ cells, and its loss in $MGMT^-$ cells, however, now allows focus on how the processes of methylation, nucleosome formation, and transcription factor binding interrelate.

While the present studies provide a more precise framework for the understanding of CpG island-containing gene silencing, they leave a number of questions unanswered. At present it remains unclear whether all human CpG island-containing genes display a precise chromatin structure and whether this chromatin structure is altered in a similar way during the gene inactivation process. The described distinction between the silencing mechanism of the X-linked HPRT gene and the somatic MGMT gene suggests that there may be multiple ways in which methylation, chromatin structure, and gene expression interact and that these interactions may vary depending on the gene location. It also remains unclear if the nucleosomal positioning suggested in the MGMT CpG island in $MGMT^+$ cells is the cause or consequence of transcription factor binding. Recent studies in this and other laboratories have shown that retention of chromatin structure is not dependent on transcription factor binding (15, 24, 31). In these studies, cells were exposed to nocodazole, resulting in mitotic arrest and transcriptional arrest as a result of transcription factor sequestration. Despite the lack of transcription factor binding in the MGMT CpG island of mitotically arrested $MGMT^+$ cells, the normal pattern of nuclease accessibility of the CpG island was retained (31). Therefore, the potential nucleosome positioning noted in the MGMT CpG island of $MGMT^+$ cells is not completely fluid but appears to be set at least by the time of mitosis. Other studies with yeast, however, have suggested that in the period between S phase and M phase, the chromatin structure is changeable, with the ultimate structure being the result of a competition between histones and transcription factors for DNA binding (3). Precise positioning of nucleosome-like structures normally seen in CpG islands such as the MGMT CpG island may therefore represent the normal outcome of this competition, while perturbations of the competition process such as alterations in cell cycle progression may tip the balance against transcription factor binding. In this sense, the nucleosomal positioning suggested in the MGMT CpG island may be neither the cause nor the consequence of transcription factor binding but, rather, may be the result of a process in which numerous outcomes are possible. Finally, and most importantly, it remains unclear what determines the positioning of nucleosome-like structures in CpG islands and what triggers alterations in this placement. A more accurate picture of the appearance of normal and aberrantly silenced CpG islands at the chromatin level may now allow these questions to be addressed in a more meaningful, biologically relevant way.

ACKNOWLEDGMENTS

We thank Joe Costello, Bernie Futscher, and George Watts for materials and helpful discussion of the manuscript.

This work was supported by Public Health Service grant CA-55064 from the National Cancer Institute.

REFERENCES

1. **Antequera, F., and A. Bird.** 1993. Number of CpG islands and genes in human and mouse. Proc. Natl. Acad. Sci. USA **90:**11995–11999.
2. **Antequera, F., J. Boyes, and A. Bird.** 1990. High levels of de novo methylation and altered chromatin structure at CpG islands in cell lines. Cell **62:**503–514.
3. **Aparicio, O. M., and D. E. Gottschling.** 1994. Overcoming telomeric silencing: a trans-activator competes to establish gene expression in a cell cycle-dependent way. Genes Dev. **8:**1136–1146.
4. **Cockell, M., D. Rhodes, and A. Klug.** 1983. Location of primary sites of micrococcal nuclease cleavage on the nucleosome core. J. Mol. Biol. **170:** 423–446.
5. **Costello, J. F., B. W. Futscher, K. Tano, D. M. Graunke, and R. O. Pieper.** 1994. Graded methylation in the promoter and body of O^6-methylguanine-DNA-methyltransferase (MGMT) gene correlates with MGMT expression in human glioma cells. J. Biol. Chem. **269:**17228–17237.

6. **Costello, J. F., B. W. Futscher, R. A. Kroes, and R. O. Pieper.** 1994. Methylation-related chromatin structure is associated with exclusion of transcription factors from and suppressed expression of the O^6-methylguanine-DNA-methyltransferase gene in human glioma cell lines. Mol. Cell. Biol. **14:**6515–6521.
7. **Drew, H. R.** 1984. Structural specificities of five commonly used DNA nucleases. J. Mol. Biol. **176:**535–557.
8. **Erickson, L. C.** 1991. The role of O-6 methylguanine DNA methyltransferase (MGMT) in drug resistance and strategies for its inhibition. Semin. Cancer Biol. **2:**257–265.
9. **Feinberg, A., and B. Vogelstein.** 1984. A technique for radiolabeling DNA restriction endonuclease fragments to high specific activity. Anal. Biochem. **137:**266–267.
10. **Gardiner-Garden, M., and M. Frommer.** 1987. CpG islands in vertebrate genomes. J. Mol. Biol. **196:**261–282.
11. **Godde, J. S., S. U. Kass, M. C. Hirst, and A. P. Wolffe.** 1996. Nucleosome assembly on methylated CGG triplet repeats in the fragile X mental retardation gene 1 promoter. J. Biol. Chem. **271:**24325–24328.
12. **Gross, D. S., and W. T. Garrard.** 1988. Nuclease hypersensitive sites in chromatin. Annu. Rev. Biochem. **57:**159–197.
13. **Harris, L. C., P. M. Potter, K. Tano, S. Shiota, S. Mitra, and T. P. Brent.** 1991. Characterization of the promoter region of the human O^6-methylguanine-DNA-methyltransferase gene. Nucleic Acids Res. **19:**6163–6167.
14. **Herman, J. G., F. Latif, Y. Weng, M. I. Lerman, B. Zbar, S. Liu, D. Samid, D.-S. R. Duan, J. R. Gnarra, W. M. Linehan, and S. B. Baylin.** 1994. Silencing of the VHL tumor-suppressor gene by DNA methylation in renal carcinoma. Proc. Natl. Acad. Sci. USA **91:**9700–9704.
15. **Hershkovitz, M., and A. D. Riggs.** 1995. Metaphase chromosome analysis by ligation-mediated PCR: heritable chromatin structure and a comparison of active and inactive X chromosomes. Proc. Natl. Acad. Sci. USA **92:**2379–2383.
16. **Issa, J.-P. J., Y. L. Ottaviano, P. Celano, S. R. Hamilton, N. E. Davidson, and S. B. Baylin.** 1994. Methylation of the oestrogen receptor CpG island links ageing and neoplasia in human colon. Nat. Genet. **7:**536–540.
17. **Kass, S. U., J. P. Gaddard, and R. L. P. Adams.** 1993. Inactive chromatin spreads from a focus of methylation. Mol. Cell. Biol. **13:**7372–7379.
18. **Kass, S. U., N. Landsberger, and A. P. Wolffe.** 1997. DNA methylation directs a time-dependent repression of transcription initiation. Curr. Biol. **7:**157–165.
19. **Kovesdi, I., R. Reichel, and J. R. Nevins.** 1987. Role of an adenovirus E2 promoter binding factor in E1A-mediated coordinate gene control. Proc. Natl. Acad. Sci. USA **84:**2180–2184.
20. **Lapidus, R. G., A. T. Ferguson, Y. L. Ottaviano, F. F. Parl, H. S. Smith, S. A. Weitzman, S. B. Baylin, J.-P. J. Issa, and N. E. Davidson.** 1996. Methylation of estrogen and progesterone receptor gene 5′ CpG islands correlates with lack of estrogen and progesterone receptor gene expression in breast tumors. Clin. Cancer Res. **2:**805–810.
21. **Larsen, F., G. Gundersen, R. Lopez, and H. Prydz.** 1992. CpG islands as gene markers in the human genome. Genomics **13:**1095–1107.
22. **Lee, W.-H., R. A. Morton, J. I. Epstein, J. D. Brooks, P. A. Campbell, G. S. Bova, W.-S. Hseih, W. B. Isaacs, and W. G. Nelson.** 1994. Cytidine methylation of regulatory sequences near the pi-class glutathione S-transferase gene accompanies human prostatic carcinogenesis. Proc. Natl. Acad. Sci. USA **91:**11733–11737.
23. **Macleod, D., J. Charlton, J. Mullins, and A. P. Bird.** 1994. Sp1 sites in the mouse aprt gene promoter are required to prevent methylation of the CpG island. Genes Dev. **8:**2282–2292.
24. **Martinez-Balbas, M. A., A. Dey, S. K. Rabindran, K. Ozato, and C. Wu.** 1995. Displacement of sequence-specific transcription factors from mitotic chromatin. Cell **83:**29–38.
25. **Maxam, A. M., and W. Gilbert.** 1980. Sequencing end-labeled DNA with base-specific chemical cleavages. Methods Enzymol. **65:**499–560.
26. **McArthur, M., and J. O. Thomas.** 1996. A preference of histone H1 for methylated DNA. EMBO J. **15:**1705–1714.
27. **Meehan, R. R., J. D. Lewis, and A. Bird.** 1992. Characterization of MeCP2, a vertebrate DNA binding protein with affinity for methylated DNA. Nucleic Acids Res. **20:**5085–5092.
28. **Meehan, R. R., J. D. Lewis, S. McKay, E. L. Kleiner, and A. Bird.** 1989. Identification of a mammalian protein that binds specifically to DNA containing methylated CpGs. Cell **58:**499–507.
29. **Miller, M. R., J. J. Castellot, and A. B. Pardee.** 1978. A permeable animal cells preparation for studying macromolecular synthesis. DNA synthesis and the role of deoxyribonucleotides in S phase initiation. Biochemistry **17:**1073–1080.
30. **Nan, X., R. R. Meehan, and A. Bird.** 1993. Dissection of the methyl-CpG binding domain from the chromosomal protein MeCP2. Nucleic Acids Res. **21:**4886–4892.
31. **Patel, S. A.** Unpublished data.
32. **Pfeifer, G. P., and A. D. Riggs.** 1991. Chromatin differences between active and inactive X chromosomes revealed by genomic footprinting of permeabilized cells using DNaseI and ligation-mediated PCR. Genes Dev. **5:**1102–1113.
33. **Pfeifer, G. P., R. L. Tanguay, S. D. Steigerwald, and A. D. Riggs.** 1990. In vivo footprint and methylation analysis by PCR-aided genomic sequencing: comparison of active and inactive X chromosomal DNA at the CpG island and promoter of human PGK-1. Genes Dev. **4:**1277–1287.
34. **Pieper, R. O., J. F. Costello, R. A. Kroes, B. W. Futscher, U. Marathi, and L. C. Erickson.** 1991. Direct correlation between methylation status and expression status and expression of the human O^6-methylguanine DNA methyltransferase gene. Cancer Commun. **3:**241–253.
35. **Pieper, R. O., S. Patel, S. A. Ting, B. W. Futscher, and J. F. Costello.** 1996. Methylation of transcription factor binding sites is unnecessary for aberrant silencing of the human MGMT gene. J. Biol. Chem. **271:**13916–13924.
36. **Qian, X. C., and T. P. Brent.** 1996. Delineation of CpG methylation sites in single copies of the MGMT gene promoter. Proc. Am. Assoc. Cancer Res. **37:**536.
37. **Rideout, W. M., III, P. Eversole-Cire, C. H. Spruck III, C. M. Hustad, G. A. Coetzee, F. A. Gonzales, and P. A. Jones.** 1994. Progressive increases in the methylation status and heterochromatinization of the *myoD* CpG island during oncogenic transformation. Mol. Cell. Biol. **14:**6143–6152.
38. **Saluz, H. P., and J. P. Jost.** 1987. A laboratory guide to sequencing, p. 11–36. Birkheuser, Boston, Mass.
39. **Tazi, J., and A. Bird.** 1990. Alternative chromatin structure at CpG islands. Cell **60:**909–920.
40. **Thomas, G. H., and S. C. R. Elgin.** 1988. Protein/DNA architecture of the DNaseI hypersensitive region of the Drosophila hsp26 promoter. EMBO J. **7:**2191–2201.
41. **Watts, G. S., and B. W. Futscher.** 1996. Hypomethylation of the O6-methylguanine DNA methyltransferase gene body eliminates its expression in a myeloma cell line. Proc. Am. Assoc. Cancer Res. **37:**537.
42. **Wijnholds, J., and G. Philipsen.** 1988. Tissue-specific and steroid-dependent interaction of transcription factors with the oestrogen-induced apoVLDL II promoter *in vivo*. EMBO. J. **7:**2757–2763.
43. **Zhang, L., and J. D. Gralla.** 1989. In situ nucleoprotein structure at the SV40 major late promoter: melted and wrapped DNA flank the start site. Genes Dev. **3:**1814–1822.
44. **Zion, M., D. Ben-Yehuda, A. Avraham, O. Cohen, M. Wetzler, D. Melloul, and Y. Ben-Neriah.** 1994. Progressive de novo DNA methylation at the bcr-abl locus in the course of chronic myelogenous leukemia. Proc. Natl. Acad. Sci. USA **91:**10722–10726.